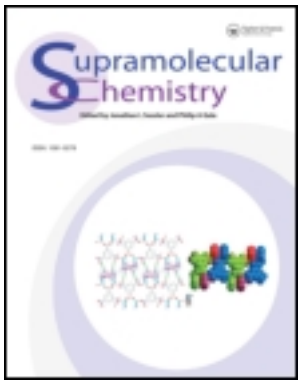

Supramolecular Chemistry
Publication details, including instructions for authors and subscription information:
http://www.tandfonline.com/loi/gsch20

Fluorescent chemosensor for biological zinc ions

Se Won Bae [a], Eunha Kim [a b], Ik-Soo Shin [a c], Seung Bum Park [a b] & Jong-In Hong [a]

[a] Department of Chemistry, Seoul National University, Seoul, 151-747, South Korea

[b] Department of Biophysics and Chemical Biology/BioMAX Institute, Seoul National University, Seoul, 151-747, South Korea

[c] Department of Chemistry, Soongsil University, Seoul, 156-743, South Korea

Published online: 20 Sep 2012.

To cite this article: Se Won Bae, Eunha Kim, Ik-Soo Shin, Seung Bum Park & Jong-In Hong (2013) Fluorescent chemosensor for biological zinc ions, Supramolecular Chemistry, 25:1, 2-6, DOI: 10.1080/10610278.2012.720020

To link to this article: http://dx.doi.org/10.1080/10610278.2012.720020

Supramolecular Chemistry
Vol. 25, No. 1, January 2013, 2–6

Taylor & Francis
Taylor & Francis Group

Fluorescent chemosensor for biological zinc ions

Se Won Bae[a], Eunha Kim[a,b], Ik-Soo Shin[a,c], Seung Bum Park[a,b]* and Jong-In Hong[a]*

[a]*Department of Chemistry, Seoul National University, Seoul 151-747, South Korea;* [b]*Department of Biophysics and Chemical Biology/BioMAX Institute, Seoul National University, Seoul 151-747, South Korea;* [c]*Department of Chemistry, Soongsil University, Seoul 156-743, South Korea*

(*Received 21 June 2012; final version received 7 August 2012*)

A synthetic fluorescent sensor (sensor **1**) is developed using boron-dipyrromethene as a fluorophore and phenoxo-bridged dipicolylamine as a receptor. Sensor **1** shows a significant enhancement of fluorescent intensity and a high selectivity for Zn^{2+} over various metal cations. The electrochemical study provides a rationale for the fluorescence turn-on of sensor **1** upon complexation with Zn^{2+} by the blocking of the photo-induced electron transfer mechanism. Sensor **1** can be used to image Zn^{2+} in A549 cells.

Keywords: fluorescent sensor; zinc ion; PeT; cell imaging

Introduction

Zn^{2+} is an important divalent metal cation in biological systems, which plays a critical role in DNA synthesis, enzyme regulation, neural signal transmission and gene expression (*1–4*). While most Zn^{2+} ions are bound to proteins, the disruption of mobile Zn^{2+} is associated with a number of diseases such as ischaemia, epilepsy, Parkinson's disease, Alzheimer's disease and certain types of cancer (*5–8*). Moreover, variation in the intracellular mobile Zn^{2+} concentration is a significant factor affecting the early apoptotic process (*9–12*). Quantitative analysis of trace Zn^{2+} using a chemosensor comprising a selective analytical receptor and a sensitive fluorophore has become extremely important for environmental and biological applications. One of the most widely applied strategies for the development of effective fluorescent Zn^{2+} sensors is the fluorescent turn-on mechanism by the regulation of photo-induced electron transfer (PeT) (*13–15*). A large number of Zn^{2+} sensors have been reported so far, and significant efforts are continuing for the development of more effective sensors to understand the biologically crucial role of Zn^{2+} (reviews: *16–20*, selected recent examples: *21–25*).

In this article, we describe the design, mechanism and evaluation of the Zn^{2+} fluorescent chemosensor, sensor **1** (Scheme 1). The selectivity and the sensitivity of sensor **1** for Zn^{2+} were examined. The fluorescence turn-on of sensor **1** upon the addition of Zn^{2+} is explained by the blocking of PeT from the electron donor. The utility of sensor **1** for Zn^{2+} sensing was demonstrated through the imaging of intracellular Zn^{2+} in A549 cells using fluorescent microscopy.

Results and discussion

First, the fluorescence emission changes of sensor **1** (1 μM) were measured as a function of Zn^{2+} (perchlorate salt) concentration. Upon the addition of Zn^{2+}, the fluorescence emission intensity of sensor **1** gradually increased. When 10 equiv. of Zn^{2+} were added to sensor **1**, the emission intensity ratio (I/I_0) showed a 4.5-fold enhancement (Figure 1).

The selectivity of sensor **1** for Zn^{2+} over other metal ions was evaluated. The experimental results show that the existence of a 10-fold excess of Li^+, Na^+, K^+, Ca^{2+}, Mn^{2+}, Fe^{2+}, Co^{2+}, Ni^{2+}, Cu^{2+}, Ag^+, Cd^{2+}, Hg^{2+} or Pb^{2+} causes fluorescence quenching (Li^+, Ca^{2+}, Mn^{2+}, Fe^{2+}, Co^{2+}, Ni^{2+}, Cu^{2+}, Ag^+, Cd^{2+}, Hg^{2+} and Pb^{2+}) or no fluorescence change (Na^+ and K^+), and that only Zn^{2+} leads to fluorescence enhancement (Figure 2).

To demonstrate the preferential binding ability of sensor **1** to Zn^{2+} over other transition metal ions, we prepared a 1 μM solution of sensor **1** with a 10-fold excess of various transition metal ions. The change in fluorescence intensity upon the addition of Zn^{2+} was measured (Figure 3). In the presence of various metal ions, the fluorescence intensity of sensor **1** decreased compared to its initial fluorescence intensity. When 10 equiv. of Zn^{2+} ions were added to the solution, the fluorescence intensity ratio showed a ninefold enhancement. The increase in fluorescence intensity upon treatment with Zn^{2+} ions is attributed to the binding of Zn^{2+} to the nitrogen atoms and a phenolate oxygen atom in sensor **1**. This, in turn, blocked the PeT, resulting in an increase in the fluorescence intensity. The fluorescence turn-on mechanism was rationalised by electrochemical studies (Figure 4). The

*Corresponding authors. Email: sbpark@snu.ac.kr; jihong@snu.ac.kr

ISSN 1061-0278 print/ISSN 1029-0478 online

http://dx.doi.org/10.1080/10610278.2012.720020
http://www.tandfonline.com

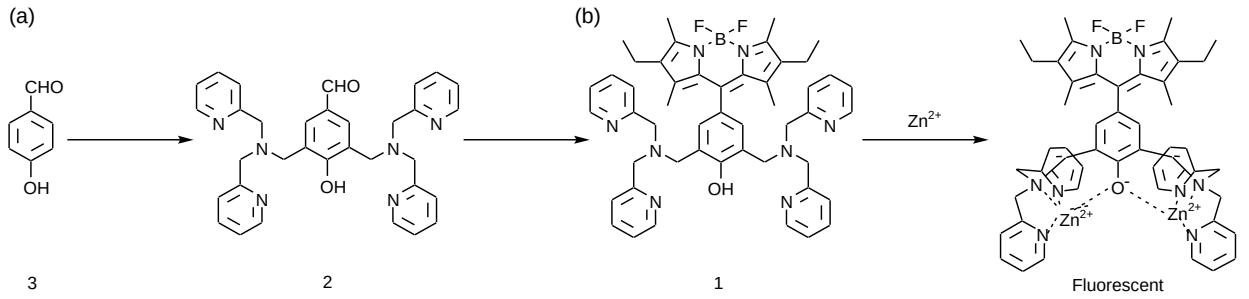

Scheme 1. Synthetic procedure for sensor **1**. (a) DPA, formaldehyde solution (37 wt%), cat. HCl, ethanol, reflux. (b) (i) 2,4-Dimethyl-3-ethylpyrrole, cat. trifluoroacetic acid (TFA), 2,3-dichloro-5,6-dicyanobenzoquinone (DDQ), CH_2Cl_2, rt; (ii) BF_3-OEt_2, TEA, CH_2Cl_2, rt.

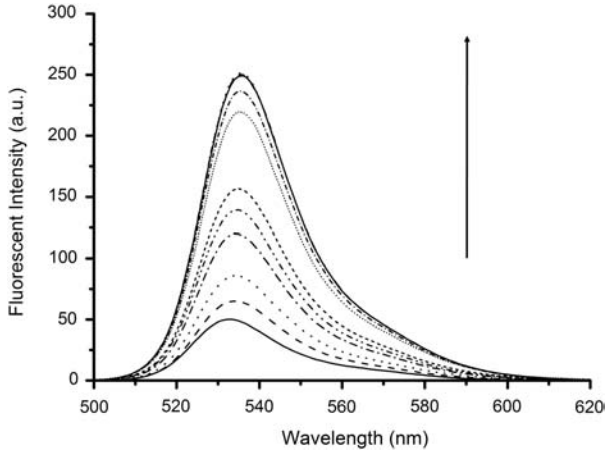

Figure 1. Changes in the fluorescence intensity of sensor **1** (1 μM) in acetonitrile upon addition of increasing amounts of Zn^{2+} (excitation at 490 nm). The arrow indicates the direction of $[Zn^{2+}]$ increase; $[Zn^{2+}] = 0$, 0.2, 0.4, 0.9, 1.3, 1.8, 3.0, 4.0, 5.0, 7.0 and 10 μM.

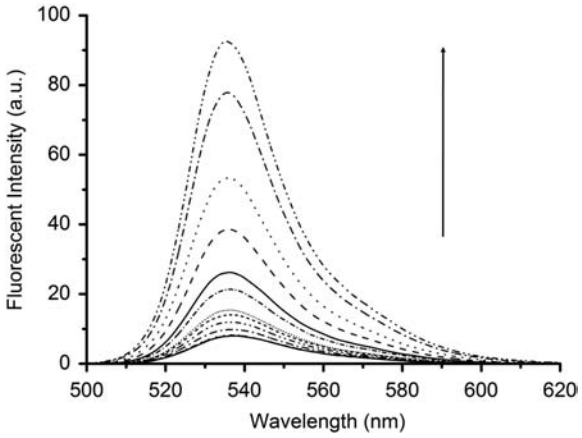

Figure 3. Changes in the fluorescence intensity of sensor **1** (1 μM) and various cations (perchlorate salts of Li^+, Na^+, K^+, Ca^{2+}, Mn^{2+}, Fe^{2+}, Co^{2+}, Ni^{2+}, Cu^{2+}, Ag^+, Cd^{2+}, Hg^{2+}, Pb^{2+} ions, 10 μM each) upon addition of increasing amounts of Zn^{2+} (perchlorate salt) in acetonitrile at 25°C. The arrow indicates the direction of $[Zn^{2+}]$ increase; $[Zn^{2+}] = 0$, 0.2, 0.4, 0.9, 1.3, 1.8, 3.0, 4.0, 5.0, 7.0 and 10 μM.

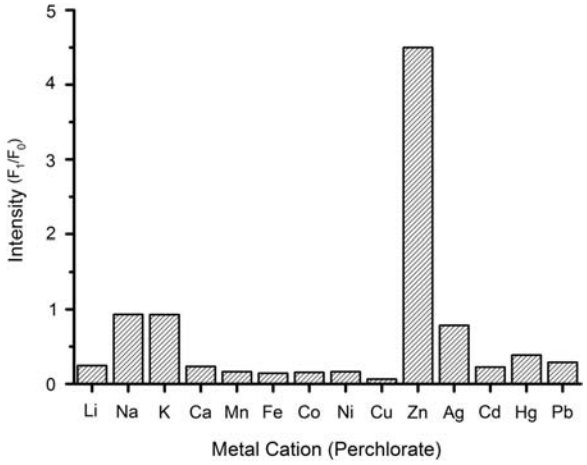

Figure 2. Relative fluorescence intensity profiles of sensor **1** (1 μM) in acetonitrile in the presence of various cations (10 equiv.). Excitation wavelength was set at 490 nm and emission was monitored at 536 nm.

obtained electrochemical data explain the changes in fluorescence intensity upon the addition of Zn^{2+} to sensor **1**. When Zn^{2+} binds to sensor **1**, there is a decrease in the electron density on the two nitrogen atoms of the amine moiety. This leads to the stabilisation of the highest occupied molecular orbital (HOMO) of sensor **1**. In order to investigate the variations in the HOMO of sensor **1**, we measured the oxidation potential of 2,6-bis((bis(pyridin-2-ylmethyl)amino)methyl)phenol (DiDPA) (see Scheme 2 for the structure of DiDPA) before and after the addition of Zn^{2+} ions. As shown in Figure 4, the first oxidation potential of DiDPA ($E_{1/2} = 0.83$ V) corresponds to the HOMO level of the amine moiety in DiDPA, and this potential becomes more positive ($E_{1/2} = 1.17$ V) upon the addition of Zn^{2+}. The incorporation of Zn^{2+} into the DiDPA moiety leads to the stabilisation of the HOMO of DiDPA through a decrease in the electron density on the DiDPA nitrogen atoms, and hence, the oxidation potential becomes more positive.

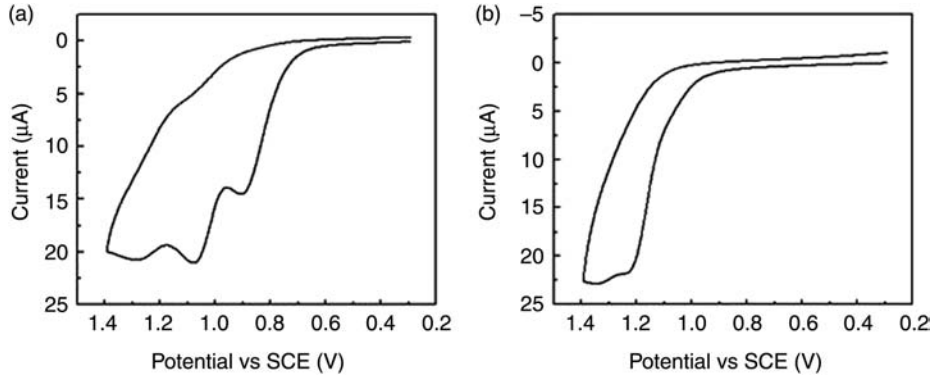

Figure 4. Cyclic voltammograms of (a) 2 mM DiDPA molecule and (b) 2 mM DiDPA after addition of 2 mM Zn^{2+} (with 0.2 M $TBAPF_6$ supporting electrolyte in acetonitrile).

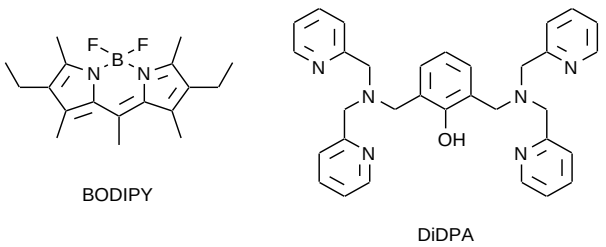

Scheme 2. Chemical structures of Bodipy and DiDPA.

On the basis of the electrochemical data, the enhancement of the fluorescence intensity can be explained from a thermodynamics viewpoint (Scheme 3). The electronic states of sensor **1** correspond to those of boron-dipyrromethene (Bodipy) and DiDPA. Since these two moieties are bonded in an orthogonal fashion, their electronic states are independent of each other, and thus, only intramolecular through-space electron transfer is allowed. Therefore, in the absence of Zn^{2+}, an electron can

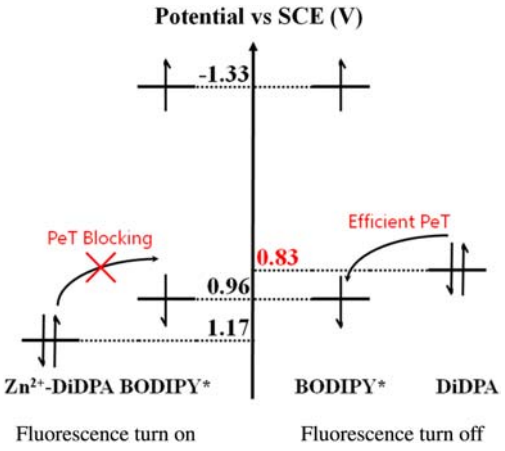

Scheme 3. Thermodynamic explanation of fluorescent enhancement upon Zn^{2+} addition to sensor **1**. Energetic values of Bodipy show a slight shift when this moiety is incorporated into sensor **1**.

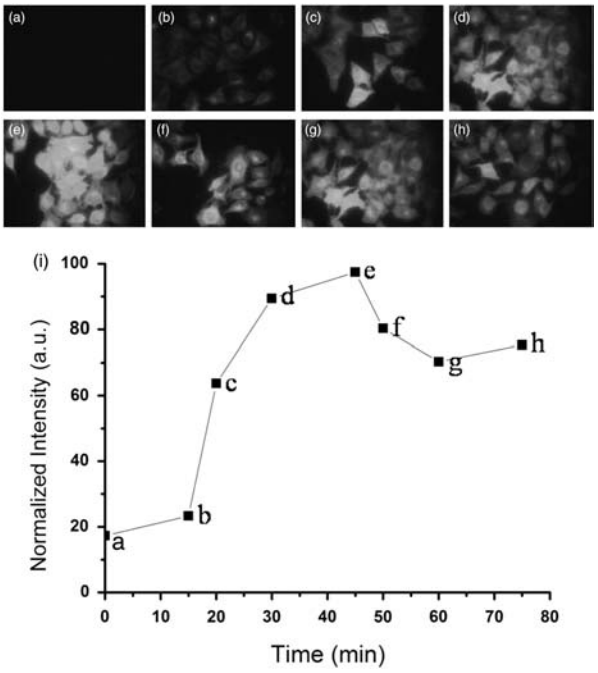

Figure 5. Fluorescence microscopy images (600 ×) of A549 cells, incubated without (a) and with (b) 10 μM sensor **1** for 30 min. Increased fluorescence signal is observed with the addition of 50 μM $ZnCl_2$ and 10 μM 2-pyrithione according to incubation time: 5 min (c), 15 min (d) and 30 min (e). TPEN addition induces the decrease in fluorescence signal according to incubation time: 5 min (f), 15 min (g) and 30 min (h). Quantification of the fluorescence intensity according to time (i).

be transferred easily from the HOMO of DiDPA to the half-filled ground state of the excited Bodipy* moiety, which subsequently leads to the efficient fluorescent quenching of sensor **1**. In the presence of Zn^{2+}, however, the HOMO of DiDPA is stabilised because of a decrease in the electron density on the nitrogen atoms of the DiDPA moiety. Hence, upon the addition of Zn^{2+}, fluorescence enhancement occurs through the blocking of PeT from the HOMO of DiDPA to the half-filled ground state of the excited Bodipy* moiety.

The fidelity of sensor **1** for the sensing of Zn^{2+} in biological systems was examined with fluorescence microscope images obtained using A549 cells (Figure 5). The cells were seeded on a cover-glass-bottomed Petri dish and incubated overnight. The cells were then washed with phosphate-buffered saline (PBS buffer) solution for 5 min each, and sensor **1** (10 μM in PBS buffer) was treated for 30 min. Then, 2-pyrithione (10 μM) and $ZnCl_2$ (50 μM) were added. The fluorescence signal was measured at each time point. After 30 min, N,N,N′,N′-tetrakis(2-pyridylmethyl)ethylenediamine (TPEN) (100 μM) was added to the A549 cells without washing, and the fluorescence signal was measured at each time point. The strong intracellular fluorescence of sensor **1** was observed until the well-known metal chelator, TPEN, induced the decrease in the fluorescence signal. Figure 5(i) shows the quantification of the fluorescence intensity according to the time domain.

Conclusion

In summary, sensor **1** binds to Zn^{2+} ions in preference to other transition metal ions. Hence, it can be used to quantify the concentration of Zn^{2+} in the presence of other transition metal ions. Furthermore, electrochemical studies reveal that the fluorescence intensity of sensor **1** increases upon the addition of Zn^{2+} through blocking of PeT from the HOMO of DiDPA to the half-filled ground state of the excited Bodipy * moiety. We have also shown that sensor **1** can image the intracellular Zn^{2+} of A549 cells. This approach is expected to be relevant to various biomedical applications, and may lead to an improved understanding of intracellular Zn^{2+}.

Experimental details

Synthesis of sensor 1

Sensor **1** was prepared according to the reported procedure (*26*). Briefly, 5.9 g of 37% aqueous formaldehyde solution was added to ethanol and then to a catalytic amount of HCl. Then, 2,2′-dipicolylamine (DPA, 11.8 mL) was added to this solution. The reaction mixture was heated at reflux for 1 day. Subsequently, 4 g of 4-hydroxybenzaldehyde was added to the reaction mixture. After stirring for 2 days at reflux, the reaction mixture was cooled to room temperature and concentrated *in vacuo* to remove all volatiles. The residue was subjected to silica column chromatography (CH_2Cl_2/MeOH) to give the desired product **2** (8.6 g, yield 48%).

Compound **2** (654 mg, 1.2 mmol) and 2,4-dimethyl-3-ethylpyrrole (0.32 mL, 2.4 mmol) were dissolved in 50 mL of absolute CH_2Cl_2 under an Ar atmosphere. One drop of trifluoroacetic acid was added, and the solution was stirred at room temperature overnight. When thin-layer chromatography monitoring (silica; CH_2Cl_2) showed complete consumption of the aldehyde, a solution of 2,3-dichloro-5,6-dicyanobenzoquinone (300 mg, 1.1 mmol) in CH_2Cl_2 was added, and stirring was continued for 15 min. The reaction mixture was washed with H_2O, dried over Na_2SO_4, filtered and evaporated. The crude compound (387 mg, 0.5 mmol) and triethylamine (TEA, 1.3 mL, 9.38 mmol) were dissolved in 60 mL of absolute CH_2Cl_2 under N_2 atmosphere and stirred at room temperature for 10 min. Then, BF_3-OEt_2 (1.3 mL, 9.37 mmol) was added, and stirring was continued for 1 h. The reaction mixture was washed with H_2O and 2 N NaOH. The aqueous solution was extracted with CH_2Cl_2. The combined organic extracts were dried over Na_2SO_4, filtered and evaporated. The crude compound was purified by column chromatography over aluminium oxide (CH_2Cl_2/MeOH, 20:1) to afford a purple powder, sensor **1** (312 mg, yield 38%).

Electrochemical measurements

The electrochemical study was conducted using a CH Instruments 660 Electrochemical Analyzer (CH Instruments, Inc., Austin, TX, USA). In the electrochemical study, cyclic voltammetry and differential pulse voltammetry were performed on the individual solutions in order to investigate their electrochemical oxidative and reductive behaviours. All the electrochemical experiments were referenced with respect to an Ag/Ag^+ reference electrode. All potential values were calibrated against the saturated calomel electrode (SCE) by measuring the oxidation potential of 1 mM ferrocene (vs Ag/Ag^+) as a standard ($E°(Fc^+/Fc) = 0.424$ V vs SCE).

Acknowledgement

This work was supported by the NRF grant funded by the MEST (Grant No. 2012-0000159).

References

(1) Jiang, P. *Coord. Chem. Rev.* **2004**, *248*, 205–229.
(2) Burdette, S.C.; Lippard, S.J. *Proc. Natl. Acad. Sci. U.S.A.* **2003**, *100*, 3605–3610.
(3) Pluth, M.D.; Tomat, E.; Lippard, S.J. *Annu. Rev. Biochem.* **2011**, *80*, 333–355.
(4) Hambidge, M.; Cousins, R.J.; Costello, R.B. *J. Nutr.* **2000**, *130*, 1341S–1343S.
(5) Frederickson, C.J.; Koh, J.-Y.; Bush, A.I. *Nat. Rev. Neurosci.* **2005**, *6*, 449–462.
(6) Takeda, A.; Tamano, H. *Brain Res. Rev.* **2009**, *62*, 33–44.
(7) Sensi, S.L.; Paoletti, P.; Bush, A.I.; Sekler, I. *Nat. Rev. Neurosci.* **2009**, *10*, 780–791.
(8) Lu, M.; Fu, D. *Science* **2007**, *317*, 1746–1748.
(9) Treves, S.; Trentini, P.L.; Ascanelli, M.; Bucci, G.; DiVirgilio, F. *Exp. Cell Res.* **1994**, *211*, 339–343.

(10) Truong-Tran, A.Q.; Carter, J.; Ruffin, R.E.; Zalewski, P.D. *Biometals* **2001**, *14*, 315–330.
(11) Kimura, E.; Takasawa, R.; Tanuma, S.; Aoki, S. *Sci. STKE* **2004**, pl7, 223.
(12) Kimura, E.; Aoki, S.; Kikuta, E.; Koike, T. *Proc. Natl. Acad. Sci. U.S.A.* **2003**, *100*, 3731–3736.
(13) de Silva, A.P.; de Silva, S.A. *Chem. Commun.* **1986**, 1709–1710.
(14) de Silva, A.P.; Gunaratne, H.Q.N.; Gunnlaugsson, T.; Huxley, A.J.M.; McCoy, C.P.; Rademacher, J.T.; Rice, T.E. *Chem. Rev.* **1997**, *97*, 1515–1566.
(15) Moore, E.G.; Bernhardt, P.V.; Fürstenberg, A.; Riley, M.J.; Smith, T.A.; Vauthey, E. *J. Phys. Chem. A* **2005**, *109*, 3788–3796.
(16) Huang, Z.; Lippard, S.J. *Methods Enzymol.* **2012**, *505*, 445–468.
(17) Tomat, E.; Lippard, S.J. *Curr. Opin. Chem. Biol.* **2010**, *14*, 225–230.
(18) Carol, P.; Sreejith, S.; Ajayaghosh, A. *Chem. Asian J.* **2007**, *2*, 338–348.
(19) Callan, J.F.; de Silva, A.P.; Magri, D.C. *Tetrahedron* **2005**, *61*, 8551–8588.
(20) Kikuchi, K.; Komatsu, K.; Nagano, T. *Curr. Opin. Chem. Biol.* **2004**, *8*, 182–191.
(21) Sun, F.; Zhang, G.; Zhang, D.; Xue, L.; Jiang, H. *Org. Lett.* **2011**, *13*, 6378–6381.
(22) Buccella, D.; Horowitz, J.A.; Lippard, S.J. *J. Am. Chem. Soc.* **2011**, *133*, 4101–4114.
(23) Iyoshi, S.; Taki, M.; Yamamoto, Y. *Org. Lett.* **2011**, *13*, 4558–4561.
(24) Du, P.; Lippard, S.J. *Inorg. Chem.* **2010**, *49*, 10753–10755.
(25) Tamanini, E.; Katewa, A.; Sedger, L.M.; Todd, M.H.; Watkinson, M. *Inorg. Chem.* **2009**, *48*, 319–324.
(26) Shin, I.-S.; Bae, S.W.; Kim, H.; Hong, J.-I. *Anal. Chem.* **2010**, *82*, 8259–8265.